PROCEEDINGS A

royalsocietypublishing.org/journal/rspa

Research

Cite this article: Wang B, Wei Y, Tang S, Hu G. 2025 Non-existence of propagating Rayleigh waves in extremal materials. *Proc. R. Soc. A* **481**: 20240960.
https://doi.org/10.1098/rspa.2024.0960

Received: 17 December 2024
Accepted: 28 May 2025

Subject Areas:
mechanics, wave motion, materials science

Keywords:
Rayleigh surface waves, extremal materials, soft modes, metamaterial design, wave controlling

Authors for correspondence:
Shaoqiang Tang
e-mail: maotang@pku.edu.cn
Gengkai Hu
e-mail: hugeng@bit.edu.cn

Non-existence of propagating Rayleigh waves in extremal materials

Bonan Wang[1], Yu Wei[2], Shaoqiang Tang[1] and Gengkai Hu[2]

[1]HEDPS and LTCS, School of Mechanics and Engineering Science, Peking University, Beijing 100871, People's Republic of China
[2]School of Aerospace Engineering, Beijing Institute of Technology, Beijing 100081, People's Republic of China

YW, 0000-0002-8915-1897; ST, 0000-0002-7387-5743

Extremal materials are a class of Cauchy materials with rank-deficient elastic matrix, i.e. exhibiting one or multiple zero eigenvalues and allowing energy-free deformation modes. In a previous study, we demonstrated that, in the Cauchy framework, no propagating Rayleigh wave exists when the extremal materials' principal axis is parallel to the free surface (Wei *et al.* 2024 *J. Mech. Phys. Solids* **193**, 105842. (doi:10.1016/j.jmps.2024.105842)). However, a question is raised naturally: can any extremal material support propagating Rayleigh wave? In this paper, we theoretically investigate the propagation of Rayleigh waves in any extremal materials based on the Cauchy framework. Dispersion relations and polarizations of Rayleigh waves in extremal materials are derived analytically. Designing a conservative function in the weak form, we prove the non-existence of propagating Rayleigh waves in any two-dimensional extremal materials, and calculate the corresponding Rayleigh modes analytically. Moreover, we illustrate the existence condition for propagating Rayleigh waves in special three-dimensional extremal materials analytically in a similar way. A Rayleigh wave isolator is proposed and demonstrated by using a piece of extremal material. This study provides a continuum model for exploring surface waves in any extremal materials and paves the way to stimulate applications of extremal materials for controlling surface waves.

THE ROYAL SOCIETY PUBLISHING

1. Introduction

Rayleigh waves, propagating along a free plane surface while decaying exponentially away from the surface, have long been a topic of utmost importance in seismology, non-destructive evaluation and sensitive detector development [1–8]. Their propagation characteristics in semi-infinite Cauchy elastic media have been investigated by many prominent researchers in both physics and mathematics communities since the twentieth century [1,9–14]. Many elegant methods and results are well documented. For example, Stroh put forward a unified formalism [10] suitable for any anisotropy of elasticity and brought unprecedented vigour and vitality for the study of Rayleigh waves. Based on the Stroh formalism, Barnet, Lothe and Chadwick extended and exploited the Stroh formalism by using the Barnet–Lothe integrals and the surface impedance tensor to analyse the uniqueness and existence issues of Rayleigh waves on the free surface of anisotropic linear elastic materials [15–18]. For elastic topological insulators that have attracted a lot of attention in recent years, their topological edge states can also be treated as Rayleigh waves [19–26]. However, such Rayleigh waves occur on free surfaces of artificial phononic crystals with geometry or material inhomogeneity rather than on free surface of homogeneous solids, and they are robust to disorders as well as fabrication imperfections [23,27].

In recent decades, with the development of elastic metamaterials, some constraints on elasticity tensor have been gradually relaxed. For instance, by allowing external energy exchange, or by careful microstructure design, the constraints on major [28,29] and minor [30–32] symmetry of elasticity tensor can be released. In addition, the elastic modulus can turn negative if resonance is introduced [33–35]. These extensions make continuum mechanics more powerful in characterizing complex phenomena and manipulating elastic waves in unprecedented ways.

Another important extension is to consider elastic materials with rank-deficient elasticity tensors, named as extremal materials. They are mathematically defined as elastic materials whose elasticity tensor may be represented as a 6×6 matrix using Voigt or Kelvin notation with $N \geq 1$ zero eigenvalues ([36]; see also [37]), giving rise to energy-free deformation modes (also referred to as easy deformation modes or zeros modes). According to Milton & Cherkaev [36], depending on N, the extremal materials are referred to as unimode materials ($N = 1$), bimode materials ($N = 2$), trimode materials ($N = 3$), quadramode materials ($N = 4$) and pentamode materials ($N = 5$). These materials can be constructed based on squares or beams connected by extremally thin parts [38–42] or soft materials [43]. Benefiting from their elasticity tensors being no longer positive definite, extremal materials show exotic ability in manipulating elastic/acoustic bulk waves [44], which are unavailable in conventional solids. For instance, underwater acoustic cloak [45,46], polarization tailoring [47,48], phonon polarizer [49,50], zero-refractive-index for elastic wave [44], static 'unfeelability' mechanical cloak [51], birefringent elastic metamaterials [52], low-frequency sound insulation [53,54], seismic wave alleviation [55], just to name a few. Since only the static mechanical property is used without resonance, the devices made of solid extremal elastic metamaterials are intrinsically broadbanded and are of great value in controlling elastic waves.

In a previous study [56], we demonstrated that, in the Cauchy framework, Rayleigh waves cannot propagate in two-dimensional extremal materials when the principal material axis is parallel to the free planar surface. While this is a very specific case, one naturally raises the question: do all extremal materials fail to support the propagating Rayleigh waves, and what are their characteristics? In this study, we follow the Stroh formalism [57] to analyse Rayleigh waves in extremal materials analytically. In the previous work [56], only the case where the principal axis of the materials is parallel to the normal of free surface is considered. In such a case, we verified either the material supports Rayleigh surface waves with zero phase velocity or there is no Rayleigh surface mode. In contrast, here we explore general extremal materials, namely, $\det(C_{ij}) = 0$, and obtain stronger conclusions.

More precisely, we focus on the study of Rayleigh waves of extremal materials in the Cauchy framework, whose elasticity tensor may be represented as a two-dimensional 3×3 matrix and three-dimensional 6×6 matrix using Voigt or Kelvin notation. First, we design

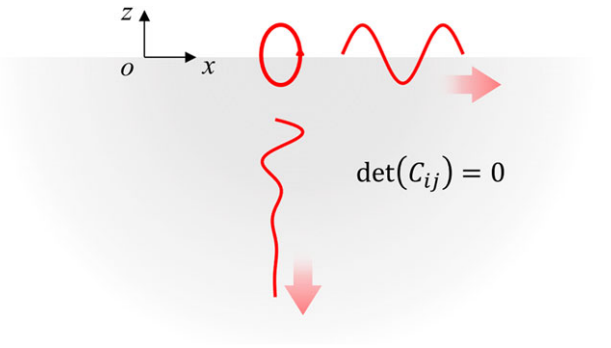

Figure 1. Schematic plot of Rayleigh surface waves propagating on the free surface of a semi-infinite elastic material in two dimensions.

Table 1. Material types and Rayleigh modes in two-dimensional extremal materials.

material type	elastic matrices	case	Rayleigh modes
unimode	$\mathbf{C}=\begin{bmatrix} a^2 & e & f \\ e & b^2 & g \\ f & g & d^2 \end{bmatrix}$	$\det(\mathbf{T})\neq 0$	$\mathbf{u}=\begin{bmatrix} -g\xi^* - \mathrm{i}d^2 \\ d^2\xi^* + \mathrm{i}f \end{bmatrix}\exp(\xi^* kz + \mathrm{i}kx),\ c=0$ $\xi^*=\frac{\sqrt{-\Delta}}{2\lvert b^2d^2-g^2\rvert}-\mathrm{i}\frac{fb^2-eg}{2(b^2d^2-g^2)}$
	$\mathbf{C}=\begin{bmatrix} a^2 & 0 & 0 \\ 0 & b^2 & 0 \\ 0 & 0 & 0 \end{bmatrix}$	$\det(\mathbf{T})=0$	$\mathbf{u}=\begin{bmatrix} \hat{u}_1 \\ 0 \end{bmatrix}\exp(\xi kz + \mathrm{i}k(x-ct)),\ \rho c^2=a^2$
biomode	$\mathbf{C}=\begin{bmatrix} a^2 & ab & ad \\ ab & b^2 & bd \\ ad & bd & d^2 \end{bmatrix}$	$\det(\mathbf{T})=0$	$\mathbf{u}=\begin{bmatrix} b\xi + \mathrm{i}d \\ -d\xi - \mathrm{i}a \end{bmatrix}\exp(\xi kz + \mathrm{i}kx),\ c=0$
	$\mathbf{C}=\begin{bmatrix} a^2 & 0 & 0 \\ 0 & 0 & 0 \\ 0 & 0 & 0 \end{bmatrix}$	$\det(\mathbf{T})=0$	$\mathbf{u}=\begin{bmatrix} \hat{u}_1 \\ 0 \end{bmatrix}\exp(\xi kz + \mathrm{i}k(x-ct)),\ \rho c^2=a^2$
else			no Rayleigh mode

a conservative function by choosing a special test function in the weak form. Using this function, we prove the non-existence of propagating Rayleigh waves in two-dimensional extremal materials. We further calculate the corresponding Rayleigh modes analytically. Then we illustrate the existence condition of propagating Rayleigh waves in special three-dimensional extremal materials analytically. In three dimensions, we prove that there is no propagating Rayleigh wave in pentamode and quadramode materials, in trimode materials when the rank of characteristic force vectors (CFVs) is 3. Finally, a Rayleigh wave isolator, which blocks the propagation of surface waves on a solid free surface is showcased.

We summarize the material types and Rayleigh modes in two-dimensional extremal materials in table 1, and those for three-dimensional extremal materials in table 2. Here, we assume $k>0$ and $\mathrm{Re}(k\xi)>0$.

The rest of this paper is organized as follows. In §2, we demonstrate that propagating Rayleigh waves cannot survive in any two-dimensional extremal materials in the Cauchy framework. The dispersion relations and polarizations are also derived analytically in detail. In §3, we illustrate

royalsocietypublishing.org/journal/rspa Proc. R. Soc. A 481: 20240960

Table 2. Material types and Rayleigh modes in three-dimensional extremal materials.

material type	elasticity matrices	case	Rayleigh modes
pentamode	$C_{ijkl}=S^{(1)}_{ij}S^{(1)}_{kl}$	$\mathrm{rank}(\mathbf{S}_3)=1$	$\mathbf{u}=\hat{\mathbf{A}}_1\exp(\xi kz+\mathrm{i}kx), c=0$
			$(\mathbf{S}_3\xi+i\mathbf{S}_1)\hat{\mathbf{A}}_1=0$
		$\mathrm{rank}(\mathbf{S}_3)=0$	$\mathbf{u}_1=\begin{bmatrix}-S_{12}A_1\exp(\xi_1 kz)\\ S_{11}A_1\exp(\xi_1 kz)\\ A_2\exp(\xi_2 kz)\end{bmatrix}\exp(\mathrm{i}kx),\quad c=0,$ or
			$\mathbf{u}_2=\begin{bmatrix}S_{11}\\ S_{12}\\ 0\end{bmatrix}\exp(\xi kz)\exp(\mathrm{i}k(x-ct)),$ $\rho c^2=S_{11}^2+S_{12}^2,$
quadramode	$C_{ijkl}=\sum_{r=1}^{2}S^{(r)}_{ij}S^{(r)}_{kl},$	$\mathrm{rank}(\mathbf{S}_3)=2$	$\mathbf{u}=\hat{\mathbf{A}}_1\exp(\xi kz+\mathrm{i}kx), c=0$
			$(\mathbf{S}_3\xi+i\mathbf{S}_1)\hat{\mathbf{A}}_1=0$
		$\mathrm{rank}(\mathbf{S}_3)=1$ *or* 0	no propagating Rayleigh wave standing (Rayleigh modes are omitted here)
trimode	$C_{ijkl}=\sum_{r=1}^{3}S^{(r)}_{ij}S^{(r)}_{kl},$	$\mathrm{rank}(\mathbf{S}_3)=3$	no propagating Rayleigh wave standing (Rayleigh modes are omitted here)
		else	may exist propagating Rayleigh waves.
unimode or biomode			may exist propagating Rayleigh waves

the existence condition of Rayleigh waves in three-dimensional extremal materials. In §4, a Rayleigh wave isolator is proposed and demonstrated, using both continuum and discrete model as an application. Finally, we summarize the main findings of this work in §5.

2. Two-dimensional general anisotropic extremal materials

Consider Rayleigh surface waves in a homogeneous Cauchy elastic material, propagating along a free surface $z=0$, as shown in figure 1. In the Cartesian coordinate system $\{x,z\}$, the motion is governed by

$$\sigma_{ij,j}=\rho\frac{\partial^2 u_i}{\partial t^2},\quad \sigma_{ij}=C_{ijkl}u_{k,l}, \tag{2.1}$$

where σ_{ij} is the symmetric stress tensor, ρ the mass density, u_i the displacement, t the time and C_{ijkl} the fourth-order elasticity tensor, respectively. The indices $i, j, k, l\in\{x,z\}$ are also denoted as $\{1,2\}$ without making any confusion. Repeated ones denote Einstein summation. The comma in $u_{k,l}$ denotes partial differentiation.

For a two-dimensional general anisotropic Cauchy material in Voigt or Kelvin notation, the elasticity matrix takes the form

$$\mathbf{C}=\begin{bmatrix}a^2 & e & f\\ e & b^2 & g\\ f & g & d^2\end{bmatrix}, \tag{2.2}$$

where $a^2=C_{1111}$, $b^2=C_{2222}$, $d^2=C_{1212}$, $e=C_{1122}$, $f=C_{1112}$ and $g=C_{2212}$ are any real numbers that make $\det(\mathbf{C})\geq 0$ hold. Instead of a positive definite $\mathbf{C}$ for traditional materials, extremal materials

royalsocietypublishing.org/journal/rspa Proc. R. Soc. A 481: 20240960

are characterized by

$$\det(\mathbf{C}) = a^2b^2d^2 + 2efg - f^2b^2 - e^2d^2 - a^2g^2 = 0. \tag{2.3}$$

Following the Stroh formalism, we define $T_{ik} = C_{i2k2}$, $R_{ik} = C_{i1k2}$, $Q_{ik} = C_{i1k1}$. This gives rise to three matrices [58]

$$\mathbf{T} = \begin{bmatrix} d^2 & g \\ g & b^2 \end{bmatrix}, \ \mathbf{R} = \begin{bmatrix} f & e \\ d^2 & g \end{bmatrix} \text{ and } \mathbf{Q} = \begin{bmatrix} a^2 & f \\ f & d^2 \end{bmatrix}. \tag{2.4}$$

In the semi-infinite elastic material ($z < 0$), displacement of a Rayleigh mode takes the form $\mathbf{u} = \hat{\mathbf{u}} e^{k\xi z} e^{ik(x-ct)}$ with $\mathrm{Re}(\xi) > 0$ [11], where k denotes the wavenumber, $i = \sqrt{-1}$ the imaginary unit, c the phase velocity and ξ the decay factor. Instead of one single mode, we consider a possible total evanescent mode with displacement

$$\mathbf{u} = \begin{bmatrix} U(kz) \\ V(kz) \end{bmatrix} \exp(\mathrm{i}k(x - ct)) = \mathbf{A}(kz) \exp(\mathrm{i}k(x - ct)). \tag{2.5}$$

The amplitude vector $\mathbf{A}(kz)$ is governed by the following ordinary differential equations [59]:

$$\mathbf{T}\mathbf{A}'' + i(\mathbf{R}+\mathbf{R}^{\mathrm{T}})\mathbf{A}' - \mathbf{Q}_c\mathbf{A} = \mathbf{0}. \tag{2.6}$$

Here and in the sequel, kz is taken as the independent variable, and $(\cdot)' = \mathrm{d}(\cdot)/\mathrm{d}(kz)$. $\mathbf{Q}_c = \mathbf{Q} - \rho c^2 \mathbf{I}$, where $\mathbf{I}$ is the identity matrix.

For the evanescent wave, it holds that

$$\lim_{z\to-\infty} \mathbf{A}(kz) = \lim_{z\to-\infty} \mathbf{A}'(kz) = \mathbf{0}. \tag{2.7}$$

In addition, the traction-free condition

$$t_i = C_{ijkl} u_{k,l} n_j = 0, at\ z = 0, \tag{2.8}$$

with the normal vector $\mathbf{n} = [0, 1]^{\mathrm{T}}$ leads to

$$\mathbf{T}\mathbf{A}'(0) + i\mathbf{R}^{\mathrm{T}}\mathbf{A}(0) = \mathbf{0}. \tag{2.9}$$

Consider the weak form of equation (2.1)

$$\int_\Omega \left(C_{ijkl}\bar{u}_{k,jl} - \rho \frac{\partial^2 \bar{u}_i}{\partial t^2} \right) \delta v_i \mathrm{d}\Omega = 0, \tag{2.10}$$

where Ω is any control volume, and δv_i is the test function. In particular, we choose $\Omega = [-\pi/k, \pi/k] \times (-\infty, kz]$ and $\delta v_i = u_{i,2}$. Then, the weak form yields

$$\int_\Omega \left(C_{ijkl}\bar{u}_{k,jl} - \rho \frac{\partial^2 \bar{u}_i}{\partial t^2} \right) u_{i,2} d\Omega = 0. \tag{2.11}$$

Using

$$\begin{aligned}
&\mathbf{A}' \cdot \mathbf{T}\overline{\mathbf{A}}'' = (\mathbf{A}' \cdot \mathbf{T}\overline{\mathbf{A}}')' - \mathbf{A}'' \cdot \mathbf{T}\overline{\mathbf{A}}' = (\mathbf{A}' \cdot \mathbf{T}\overline{\mathbf{A}}')' - \bar{\mathbf{A}}' \cdot \mathbf{T}\mathbf{A}'', \\
&\mathbf{A}' \cdot (\mathbf{R}+\mathbf{R}^{\mathrm{T}})\overline{\mathbf{A}}' = \overline{\mathbf{A}}' \cdot (\mathbf{R}+\mathbf{R}^{\mathrm{T}})\mathbf{A}', \\
&\mathbf{A}' \cdot \mathbf{Q}_c\overline{\mathbf{A}} = (\mathbf{A} \cdot \mathbf{Q}_c\overline{\mathbf{A}})' - \mathbf{A} \cdot \mathbf{Q}_c\overline{\mathbf{A}}' = (\mathbf{A}' \cdot \mathbf{Q}_c\overline{\mathbf{A}})' - \bar{\mathbf{A}}' \cdot \mathbf{Q}_c\mathbf{A},
\end{aligned} \tag{2.12}$$

together with equation (2.6), we rewrite equation (2.11)

$$\begin{aligned}0&=\int_{-\infty}^{kz}\left(C_{ijkl}\bar{u}_{k,jl}-\rho\frac{\partial^2\bar{u}_i}{\partial t^2}\right)u_{i,2}\mathrm{d}(kz)\\&=\int_{-\infty}^{kz}\{\mathbf{T}\overline{\mathbf{A}}'^{\prime}-i(\mathbf{R}+\mathbf{R}^{\mathrm{T}})\overline{\mathbf{A}}'-\mathbf{Q}_c\overline{\mathbf{A}}\}\cdot\mathbf{A}'d(kz)\\&=\int_{-\infty}^{kz}(\mathbf{A}'\cdot\mathbf{T}\overline{\mathbf{A}}'-\mathbf{A}\cdot\mathbf{Q}_c\overline{\mathbf{A}})'-\overline{\mathbf{A}}'\cdot(\mathbf{T}\mathbf{A}''+i(\mathbf{R}+\mathbf{R}^{\mathrm{T}})\mathbf{A}'-\mathbf{Q}_c\mathbf{A})d(kz)\\&=(\mathbf{A}'\cdot\mathbf{T}\overline{\mathbf{A}}'-\mathbf{A}\cdot\mathbf{Q}_c\overline{\mathbf{A}})|_{-\infty}^{kz}.\end{aligned}\tag{2.13}$$

According to equation (2.7), the above term vanishes at $kz\to-\infty$. Therefore, the function

$$\Phi(\mathbf{A}(kz))=\mathbf{A}'\cdot\mathbf{T}\overline{\mathbf{A}}'-\mathbf{A}\cdot\mathbf{Q}_c\overline{\mathbf{A}}=0.\tag{2.14}$$

This is key to our proof for non-existence of propagating Rayleigh waves. According to the coefficient matrix in equation (2.9), we discuss two cases: one is $\det(\mathbf{T})\neq0$, the other is $\det(\mathbf{T})=0$. When $\det(\mathbf{T})\neq0$, such anisotropic material can only be a unimode material. However, when $\det(\mathbf{T})=0$, such anisotropic material can either be a bimode material or a unimode material [44].

(a) Case 1: $\det(\mathbf{T})\neq0$

Combining equations (2.3) and (2.4), we get

$$\mathbf{R}\mathbf{T}^{-1}\mathbf{R}^{T}=\mathbf{Q}.\tag{2.15}$$

Substituting equations (2.9) and (2.15) into equation (2.14) gives

$$\begin{aligned}0&=\Phi(\mathbf{A}(0))\\&=\mathbf{A}'(0)\cdot\mathbf{T}\overline{\mathbf{A}}'(0)-\mathbf{A}(0)\cdot\mathbf{Q}_c\overline{\mathbf{A}}(0)\\&=\overline{\mathbf{A}}(0)\cdot(\mathbf{R}\mathbf{T}^{-1}\mathbf{R}^{\mathrm{T}}-\mathbf{Q}_c)\mathbf{A}(0)\\&=\overline{\mathbf{A}}(0)\cdot(\mathbf{N}_3+\rho c^2\mathbf{I})\mathbf{A}(0)\\&=\rho c^2|\mathbf{A}(0)|^2\\&=\left(\frac{\rho}{k^2}\dot{\mathbf{u}}^H\dot{\mathbf{u}}\right)\Big|_{kz=0},\end{aligned}\tag{2.16}$$

where the matrix $\mathbf{N}_3=\mathbf{R}\mathbf{T}^{-1}\mathbf{R}^{T}-\mathbf{Q}$ is a significant matrix defined in the Stroh formalism [58]. Specifically, $\mathbf{N}_3=\mathbf{R}\mathbf{T}^{-1}\mathbf{R}^{T}-\mathbf{Q}=\mathbf{Q}-\mathbf{Q}=\mathbf{0}$ in this case. The kinetic energy at the surface is zero. Since $\rho\neq0$, unless $c=0$, it must hold $\mathbf{A}(0)=0$, and accordingly $\mathbf{A}'(0)=0$ as well. Then, we obtain the trivial equilibrium for equation (2.1).

Notice that the matrix $\mathbf{N}_3$ is a semi-negative definite matrix in the Stroh formalism for materials with positive definite $\mathbf{C}$ [58]. So the equation $\overline{\mathbf{A}}(0)\cdot(-\mathbf{N}_3)\mathbf{A}(0)=\rho c^2|\mathbf{A}(0)|^2$ can be regarded as the total energy of the system being equally divided between potential energy and kinetic energy at the surface. However, in extremal materials with $\det(\mathbf{T})\neq0$, equation (2.15) holds and $\mathbf{N}_3=\mathbf{0}$, which results in the potential energy and the kinetic energy both being zero at the surface.

In conclusion, propagating Rayleigh wave ($c\neq0$) does not exist in two-dimensional extremal material for the case with $\det(\mathbf{T})\neq0$.

(b) Case 2: $\det(\mathbf{T}) = 0$

This is a degenerate case, so we need to discuss in detail. According to equation (2.6), the eigen-equation for $\mathbf{A}$ reads

$$\begin{aligned} 0 &= \det(\mathbf{T}\xi^2 + i(\mathbf{R}^{\mathrm{T}}+\mathbf{R})\xi - \mathbf{Q}_c) \\ &= (b^2d^2 - g^2)\xi^4 + 2\mathrm{i}(b^2f - ge)\xi^3 + [\rho c^2(b^2+d^2) - a^2b^2 - 2fg + 2d^2e + e^2]\xi^2 \\ &\quad + 2\mathrm{i}[\rho c^2(f+g) - a^2g + ef]\xi + (\rho c^2 - a^2)(\rho c^2 - d^2) - f^2. \end{aligned} \tag{2.17}$$

In the following analysis, we are only interested in right propagating waves with $\mathrm{Re}(\xi) > 0$ to ensure that the wave decays exponentially along the $-z$-direction.

Then, combining equations (2.6), (2.7) and (2.9) yields the equation for the phase velocity c. When substituting c back into equations (2.6) and (2.17), the decay factor ξ and displacement $\mathbf{u}$ may be obtained.

Considering equation (2.3) and $\det(\mathbf{T}) = 0$, we find $bf = \pm ed$ and $fg = ed^2$. Then, both the quartic and cubic coefficients of the eigen-equation (2.17) are zero, namely

$$0 = [\rho c^2(b^2+d^2) - a^2b^2 + e^2]\xi^2 + 2\mathrm{i}[\rho c^2(f+g) - a^2g + ef]\xi + (\rho c^2 - a^2)(\rho c^2 - d^2) - f^2. \tag{2.18}$$

So there is only one partial wave for any $\mathrm{Re}(k\xi) > 0$ satisfying the requirement of equation of motions

$$\mathbf{u} = \begin{bmatrix} \hat{u}_1 \\ \hat{v}_1 \end{bmatrix} \exp(\xi kz)\exp(ik(x - ct)) = \hat{\mathbf{A}}_1 \exp(\xi kz)\exp(ik(x - ct)). \tag{2.19}$$

The amplitude of $\mathbf{u}$ is non-zero to rule out the trivial equilibrium. Inserting equation (2.19) into equations (2.6) and (2.8) yields

$$\mathbf{T}\hat{\mathbf{A}}_1\xi^2 + i(\mathbf{R}^{\mathrm{T}}+\mathbf{R})\hat{\mathbf{A}}_1\xi - \mathbf{Q}_c\hat{\mathbf{A}}_1 = 0 \tag{2.20}$$

and

$$\mathbf{T}\hat{\mathbf{A}}_1\xi + i\mathbf{R}^{\mathrm{T}}\hat{\mathbf{A}}_1 = 0, \tag{2.21}$$

respectively. Since $\rho \neq 0$, there are only three possible circumstances: either $c = 0$, or $\hat{\mathbf{A}}_1 = 0$, or $d = e = f = g = 0$ with $a \neq 0$ and $c = \sqrt{a^2/\rho}$. (See appendix A for detail.)

The first circumstance implies that the Rayleigh wave phase velocity is zero, hence not propagating. The second circumstance represents again the trivial equilibrium. The third circumstance leads to the following surface wave for any $\mathrm{Re}(k\xi) > 0$,

$$\mathbf{u} = \begin{bmatrix} \hat{u}_1 \\ 0 \end{bmatrix} \exp(\xi kz)\exp\left(ik\left(x - \sqrt{a^2/\rho}t\right)\right). \tag{2.22}$$

This is a rather special situation as the elastic tensor essentially has only one non-zero component $C_{1111} = a^2$ and the material behaves like a one-dimensional material. So, this is not regarded as a generic propagating Rayleigh wave, and we discard this case.

As a conclusion, there is no propagating Rayleigh wave in two-dimensional extremal material.

(c) Rayleigh modes

In this subsection, we will examine the characteristics of standing Rayleigh waves in extremal materials. First, we derive the surface wave displacement field for a two-dimensional general anisotropic extremal material, including its polarization and decay factor. Then, as an example to illustrate our findings, we examine the case of orthotropic extremal materials, which is oriented at an angle of θ with respect to the free plane surface.

According to equation (2.9), two cases need to be examined, i.e. $\det(\mathbf{T}) \neq 0$ or $\det(\mathbf{T}) = 0$. In this section, we discuss the first case below, while the second case is discussed in appendix A.

Substituting $c=0$ and equation (2.3) into the eigen-equation (2.17) yields

$$\frac{1}{b^2d^2-g^2}[(b^2d^2-g^2)\xi^2-(b^2f-eg)\xi-(fg-d^2e)]^2=0. \tag{2.23}$$

This quartic equation has two double roots

$$\xi_1=\xi_2=-\mathrm{i}\frac{fb^2-eg+\sqrt{\Delta}}{2(b^2d^2-g^2)}$$

and

$$\xi_3=\xi_4=-\mathrm{i}\frac{fb^2-eg-\sqrt{\Delta}}{2(b^2d^2-g^2)}, \tag{2.24}$$

where

$$\Delta=(fb^2-eg)^2-4(b^2d^2-g^2)(fg-ed^2). \tag{2.25}$$

The double root with $\mathrm{Re}(\xi)>0$ is

$$\xi^*=\xi_1=\xi_2=\frac{\sqrt{-\Delta}}{2|b^2d^2-g^2|}-\mathrm{i}\frac{fb^2-eg}{2(b^2d^2-g^2)}, \tag{2.26}$$

where $\Delta<0$. Under the traction-free condition, the wave mode takes the form

$$\mathbf{u}=\begin{bmatrix}-g\xi^*-\mathrm{i}d^2\\ d^2\xi^*+\mathrm{i}f\end{bmatrix}\exp(\xi^*kz+\mathrm{i}kx),\ c=0. \tag{2.27}$$

Interestingly, this displacement field results in null stress. In other words, the non-zero evanescent wave displacement field generates a zero stress field. Therefore, this displacement field for a unimode materials $\det(\mathbf{T})\neq 0$ represents a surface mode with zero velocity.

To illustrate the characteristics of Rayleigh wave in extremal materials, consider an example of orthotropic extremal materials whose principle axis takes an angle θ to the coordinate axis.

The elasticity matrix is

$$\mathbf{C}=\mathbf{T}_\theta\mathbf{C}_0{\mathbf{T}_\theta}^T, \tag{2.28}$$

with

$$\mathbf{C}_0=\begin{bmatrix}C_{1111}&C_{1122}&0\\ C_{1122}&C_{2222}&0\\ 0&0&C_{1212}\end{bmatrix} \tag{2.29}$$

and

$$\mathbf{T}_\theta=\begin{bmatrix}\cos^2\theta&\sin^2\theta&-\sin 2\theta\\ \sin^2\theta&\cos^2\theta&\sin 2\theta\\ \sin 2\theta/2&-\sin 2\theta/2&\cos 2\theta\end{bmatrix}. \tag{2.30}$$

Since an extremal material with $\det(\mathbf{T})\neq 0$ must be a unimode material, there are only two types of elasticity matrix $\mathbf{C}_0$ [56], namely

$$\mathbf{C}_0=\begin{bmatrix}a^2&\alpha ab&0\\ \alpha ab&b^2&0\\ 0&0&0\end{bmatrix},\ |\alpha|<1 \tag{2.31}$$

or

$$\mathbf{C}_0=\begin{bmatrix}a^2&ab&0\\ ab&b^2&0\\ 0&0&d^2\end{bmatrix}. \tag{2.32}$$

If the elasticity matrix takes the form of equation (2.31), substituting equations (2.29)–(2.31) into equation (2.25) yields

$$\Delta=\frac{1}{4}a^4b^4(1-\alpha^2)^2\sin^2 2\theta\geq 0. \tag{2.33}$$

According to equation (2.24), the wave does not decay. Hence, there is no evanescent wave or Rayleigh mode for any angle θ.

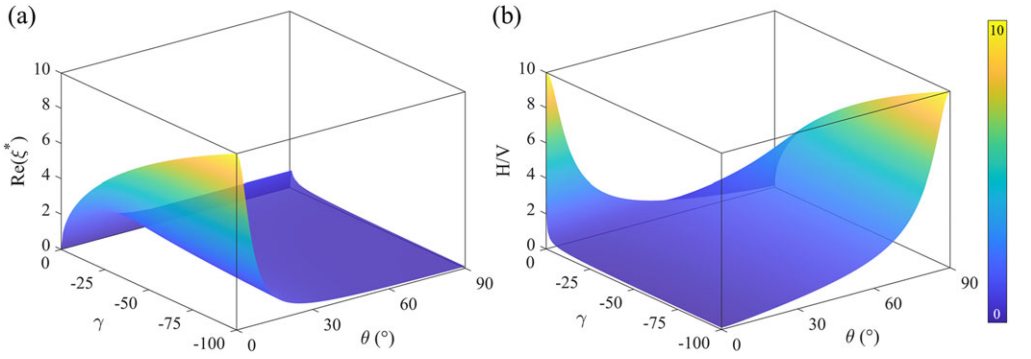

Figure 2. (a) The real part of the decay factor ξ and (b) the ellipticity ratio (H/V) for the surface particle polarization of a unimode material, under the constraint of $\det(\mathbf{T}) \neq 0$, versus Poisson's ratio γ and rotation angle θ.

On the other hand, if the elasticity matrix takes the form of equation (2.32), we denote Poisson's ratio $\gamma = a/b$ for stress in the x-direction of $\mathbf{C}_0$. Substituting equation (2.32) into equations (2.25)–(2.27) and equations (2.29), (2.30), we find the following wave mode:

$$\xi^* = \xi_1 = \xi_2 = \frac{\sqrt{-\gamma} + \mathrm{i}\frac{\gamma+1}{2}\sin 2\theta}{\cos^2\theta - \gamma\sin^2\theta},\ \gamma < 0$$
$$\mathbf{u} = \begin{bmatrix} \cos\theta + \mathrm{i}\sqrt{-\gamma}\sin\theta \\ \sin\theta - \mathrm{i}\sqrt{-\gamma}\cos\theta \end{bmatrix} \exp(\xi^* kz + \mathrm{i}kx),\ c = 0. \tag{2.34}$$

Again, this displacement field satisfies the traction-free condition, and therefore represents a surface mode with zero phase velocity in orthotropic unimode materials for any $\gamma < 0$ and any θ.

For a surface particle, denote its displacement component along the surface as H, and that perpendicular to the surface as V. The ellipticity [60]

$$H/V = \sqrt{\frac{\cos^2\theta - \gamma\sin^2\theta}{\sin^2\theta - \gamma\cos^2\theta}}, \tag{2.35}$$

represents the ratio between the surface particle's displacement component (H) along the surface and that perpendicular to the surface (V). For general parameters of θ and γ, figure 2a,b shows the Rayleigh wave decay factor (Re(ξ^*)) and the ellipticity, respectively. For any given θ, the Re(ξ^*) $\to 0$ when $\gamma \to 0$. While, when $\theta \to 0$, the real part of the decay factor Re(ξ^*) $\to \sqrt{-\gamma}$, which increases along with the decrease of γ. In figure 2b, the ellipticity (H/V) decreases as γ and θ simultaneously increase or decrease. But when γ increases and θ decreases (or γ decreases and θ increases), the ellipticity increases. This characteristic can be well explained by equation (2.35). When $\theta \to 0$, the ellipticity $H/V \to \sqrt{-1/\gamma}$ indicating the ellipticity negatively correlated to the magnitude of γ. While, when $\theta \to \pi/2$, the ellipticity $H/V \to \sqrt{-\gamma}$, indicating the ellipticity positively correlated to the magnitude of γ.

Note when $\gamma = -1$, i.e. for an isotropic unimode material, equation (2.34) is reduced to

$$\xi^* = 1,\ \mathbf{u} = \begin{bmatrix} \mathbf{i} \\ 1 \end{bmatrix} \exp(\xi^* kz + \mathrm{i}kx),\ c = 0. \tag{2.36}$$

This represents a surface mode with zero phase velocity consistent with the results in our previous work, which was verified numerically by twisted-kagome lattice [56].

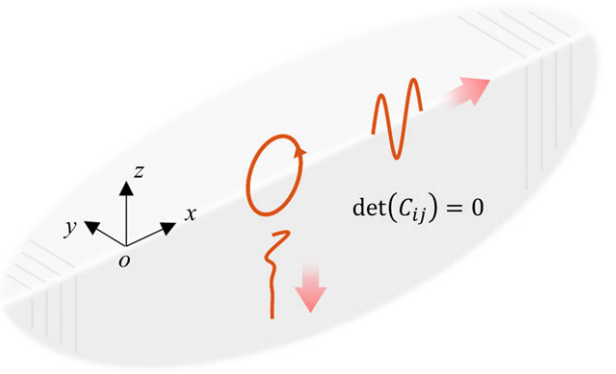

Figure 3. Scheme of Rayleigh surface waves propagating on the free surface of a semi-infinite elastic material in three dimensions.

3. Three-dimensional general anisotropic extremal materials

The behaviour of Rayleigh waves in three-dimensional extremal materials differs significantly from that in two dimensions. To complete our theory, it is essential to further investigate the behaviour of Rayleigh waves in general three-dimensional extremal materials. In this section, we discuss the Rayleigh waves in three dimensions. The schematic plot of Rayleigh waves propagating on the free surface in three dimensions is shown in figure 3.

The fourth-order elasticity tensor for an elastic material with N zero eigenvalues is expressed as

$$C_{ijkl} = \sum_{r=1}^{6-N} K_r S_{ij}^{(r)} S_{kl}^{(r)}, \tag{3.1}$$

with K_r being the non-zero eigenvalue of the elasticity tensor, and $\mathbf{S}^{(r)}$ being a second-order symmetric tensor (representing hard mode). For the sake of convenience, equation (3.1) can also be written in a compact form as $C_{ijkl} = \sum_{r=1}^{6-N} S_{ij}^{(r)} S_{kl}^{(r)} = S_{ij}^{(r)} S_{kl}^{(r)}$, in which K_r is absorbed in $\mathbf{S}^{(r)}$. Here, the repeated upper index (r) means Einstein summation. The free surface $z=0$ takes a normal $\mathbf{n} = (0,0,1)^T$. We consider evanescent waves propagating along the $+x$-direction and decaying exponentially along the $-z$-direction. As before, we define

$$T_{ik} = C_{i3k3} = S_{i3}^{(r)} S_{k3}^{(r)}, R_{ik} = C_{i1k3} = S_{i1}^{(r)} S_{k3}^{(r)}, Q_{ik} = C_{i1k1} = S_{i1}^{(r)} S_{k1}^{(r)}, \tag{3.2}$$

and additionally three $3 \times (6-N)$ matrices

$$\mathbf{S}_j = S_{ij}^r = \begin{bmatrix} S_{i1}^{(r)} \\ S_{i2}^{(r)} \\ S_{i3}^{(r)} \end{bmatrix}, j = 1,2,3, \tag{3.3}$$

which leads to

$$\mathbf{T} = \mathbf{S}_3 \mathbf{S}_3^T, \mathbf{R} = \mathbf{S}_1 \mathbf{S}_3^T, \mathbf{Q} = \mathbf{S}_1 \mathbf{S}_1^T. \tag{3.4}$$

Assume a displacement field

$$\mathbf{u} = \begin{bmatrix} U(kz) \\ V(kz) \\ W(kz) \end{bmatrix} \exp(\mathrm{i}k(x-ct)) = \mathbf{A}(kz) \exp(\mathrm{i}k(x-ct)), \tag{3.5}$$

where $\boldsymbol{A}(kz)$ is a complex-valued vector function under the constraint

$$\lim_{z \to -\infty} \mathbf{A}(kz) = \lim_{z \to -\infty} \mathbf{A}'(kz) = \mathbf{0}. \tag{3.6}$$

Similar to the two-dimensional problem, the equation of motion can be written as

$$\mathbf{T}\mathbf{A}'' + i(\mathbf{R}+\mathbf{R}^{\mathbf{T}})\mathbf{A}' - \mathbf{Q}_c\mathbf{A} = \mathbf{0}. \tag{3.7}$$

The same as in the previous section, $\mathbf{A}(kz)$ is abbreviated as $\mathbf{A}$. The prime $(')$ represents the derivative with respect to kz.

The traction-free condition in equation (2.8) at $z = 0$ still reads

$$\mathbf{T}\mathbf{A}'(0) + i\mathbf{R}^{\mathbf{T}}\mathbf{A}(0) = \mathbf{0}, \tag{3.8}$$

and similar to equation (2.13),

$$\Phi(\mathbf{A}(kz)) = \mathbf{A}' \cdot \mathbf{T}\overline{\mathbf{A}}' - \mathbf{A} \cdot \mathbf{Q}_c\overline{\mathbf{A}} = 0. \tag{3.9}$$

So, we have $\Phi(0) = 0$.

We define CFVs as

$$\mathbf{t}_i = \mathbf{S}^{(i)} \cdot \mathbf{n}, \tag{3.10}$$

representing the projection of the hard mode $\mathbf{S}^{(i)}$ on the free surface, or on the wavefront plane (whose normal is $\mathbf{n} = (0,\ 0,\ 1)^T$, cf. [44]). In our previous work, we demonstrated that CFVs may shed light on the characteristic of equi-frequency surface (i.e. the bulk wave properties of extremal materials) along the $\mathbf{n}$ direction. They also play an important role in discussing the characteristics of Rayleigh waves in extremal material. In the following, we shall use the conservative function Φ in equation (3.9) to exclude propagating Rayleigh waves in trimode ($N = 3$), quadramode ($N = 4$) and pentamode ($N = 5$) materials when

$$\operatorname{rank}(\mathbf{S}_3) = \operatorname{rank}([\mathbf{t}_1, \ldots, \mathbf{t}_{6-N}]) = 6 - N. \tag{3.11}$$

As a matter of fact, equation (3.8) can be rewritten as

$$\mathbf{S}_3\mathbf{S}_3^T\mathbf{A}'(0) + i\mathbf{S}_3\mathbf{S}_1^T\mathbf{A}(0) = 0, \tag{3.12}$$

which leads to

$$\mathbf{S}_3^T\mathbf{A}'(0) + i\mathbf{S}_1^T\mathbf{A}(0) = 0, \tag{3.13}$$

for $\ker(\mathbf{S}_3) = \{\mathbf{0}\}$. Then substituting equation (3.13) into equation (3.9), we get the conclusion similar to equation (2.16)

$$\begin{aligned}
0 &= \Phi(\mathbf{A}(0)) \\
&= \mathbf{A}'(0) \cdot \mathbf{T}\overline{\mathbf{A}}'(0) - \mathbf{A}(0) \cdot \mathbf{Q}_c\overline{\mathbf{A}}(0) \\
&= \mathbf{A}'(0) \cdot \mathbf{S}_3\mathbf{S}_3^T\overline{\mathbf{A}}'(0) - \mathbf{A}(0) \cdot \mathbf{Q}_c\overline{\mathbf{A}}(0) \\
&= \overline{\mathbf{A}}(0) \cdot (\mathbf{S}_1\mathbf{S}_1^T - \mathbf{Q}_c)\mathbf{A}(0) \\
&= \overline{\mathbf{A}}(0) \cdot (\mathbf{Q} - \mathbf{Q}_c)\mathbf{A}(0) \\
&= \rho c^2 |\mathbf{A}(0)|^2 \\
&= \left(\frac{\rho}{k^2}\dot{\mathbf{u}}^H\dot{\mathbf{u}}\right)\Big|_{kz=0}.
\end{aligned} \tag{3.14}$$

Similar to two-dimensional cases, three-dimensional extremal materials with $\operatorname{rank}(\mathbf{S}_3) = 6 - N$ take kinetic energy vanishing at the surface.

(a) Pentamode materials

According to the definition in equation (3.1), the elastic tensor of a general pentamode material is

$$C_{ijkl} = S^{(1)}_{ij} S^{(1)}_{kl},\ \mathbf{S}^{(1)} = \begin{bmatrix} S^{(1)}_{11} & S^{(1)}_{12} & S^{(1)}_{13} \\ S^{(1)}_{12} & S^{(1)}_{22} & S^{(1)}_{23} \\ S^{(1)}_{13} & S^{(1)}_{23} & S^{(1)}_{33} \end{bmatrix}, \tag{3.15}$$

i.e. $r = 1$, $N = 5$. Similar to two-dimensional cases, combining the governing equations (3.7) and traction-free condition equation (3.8), we classify two cases: $\mathrm{rank}(\mathbf{S}_3) \neq 0$ and $\mathrm{rank}(\mathbf{S}_3) = 0$.

For the case $\mathrm{rank}(\mathbf{S}_3) \neq 0$, i.e. $\mathrm{rank}(\mathbf{S}_3) = \mathrm{rank}(\mathbf{t}_1) = 1 = 6 - 5$, equation (3.14) implies that the kinetic energy vanishes at the surface. It requires $\mathbf{u}(0) = 0$ or $c = 0$. For the dynamical system, $\mathbf{u}(0) = 0$ leads to $\mathbf{u}(z) = 0$, corresponding to trivial equilibrium. Therefore, if a Rayleigh wave exists, it must be with zero phase velocity. For any $\mathrm{Re}(\xi) > 0$, it can be expressed as:

$$\mathbf{u} = \begin{bmatrix} \hat{u}_1 \\ \hat{v}_1 \\ \hat{w}_1 \end{bmatrix} \exp(\xi k z + \mathrm{i} k x) = \hat{\mathbf{A}}_1 \exp(\xi k z + \mathrm{i} k x), c = 0, \tag{3.16}$$

where $\hat{\mathbf{A}}_1$satisfies

$$(\mathbf{S}_3 \xi + i\mathbf{S}_1)\hat{\mathbf{A}}_1 = \mathbf{0}. \tag{3.17}$$

Next, we consider the case $\mathrm{rank}(\mathbf{S}_3) = 0$, i.e. $\mathbf{S}_3 = 0$. The traction-free condition is naturally satisfied. Substituting $\mathbf{S}_3 = 0$ into equation (3.7) leads to

$$\mathbf{Q}_c \hat{\mathbf{A}}_1 = \mathbf{0}. \tag{3.18}$$

If there exists a non-trivial solution of the displacement, the determinant of $\mathbf{Q}_c$ must be zero, i.e.

$$(\rho c^2)^2 [\rho c^2 - (S^2_{11} + S^2_{12})] = 0. \tag{3.19}$$

There are two possibilities, either $c = 0$ or $\rho c^2 = S^2_{11} + S^2_{12}$. They yield two bulk wave modes

$$\mathbf{u}_1 = \begin{bmatrix} -S_{12} A_1 \exp(\xi_1 k z) \\ S_{11} A_1 \exp(\xi_1 k z) \\ A_2 \exp(\xi_2 k z) \end{bmatrix} \exp(\mathrm{i} k x),\ c = 0, \tag{3.20}$$

$$\mathbf{u}_2 = \begin{bmatrix} S_{11} \\ S_{12} \\ 0 \end{bmatrix} \exp(\xi k z) \exp(\mathrm{i} k (x - ct)),\ \rho c^2 = S^2_{11} + S^2_{12}, \tag{3.21}$$

where A_1 and A_2 are arbitrary constants. The displacement field in equation (3.20) for any $\mathrm{Re}(\xi) > 0$ represents a Rayleigh mode with zero phase velocity. That in equation (3.21) represents a surface wave for any $\mathrm{Re}(\xi) > 0$ with phase velocity that is equal to the bulk wave speed, which may be a kind of limiting bulk wave [61,62]. This is a rather special situation, as the elastic tensor components are independent of the z coordinate giving rise to a three-dimensional monoclinic extremal material symmetry with respect to the (x, y)-plane. However, this material behaves like a two-dimensional material. This is similar to the case discussed in §2 where the two-dimensional material behaves like a one-dimensional material. Since we mainly focus on the Rayleigh waves whose phase velocity is smaller than those of bulk waves, we discard this case.

Therefore, there is no propagating Rayleigh wave in pentamode material.

(b) Quadramode materials

A quadramode material only has two hard modes, i.e. $r=2, N=4$. Therefore, the general elasticity tensor is

$$C_{ijkl}=S_{ij}^{(1)}S_{kl}^{(1)}+S_{ij}^{(2)}S_{kl}^{(2)},\ \mathbf{S}^{(1)}=\begin{bmatrix} S_{11}^{(1)} & S_{12}^{(1)} & S_{13}^{(1)} \\ S_{12}^{(1)} & S_{22}^{(1)} & S_{23}^{(1)} \\ S_{13}^{(1)} & S_{23}^{(1)} & S_{33}^{(1)} \end{bmatrix},\ \mathbf{S}^{(2)}=\begin{bmatrix} S_{11}^{(2)} & S_{12}^{(2)} & S_{13}^{(2)} \\ S_{12}^{(2)} & S_{22}^{(2)} & S_{23}^{(2)} \\ S_{13}^{(2)} & S_{23}^{(2)} & S_{33}^{(2)} \end{bmatrix}. \tag{3.22}$$

In this subsection, we demonstrate that the Rayleigh wave cannot propagate in quadramode material if $\mathrm{rank}(\mathbf{S}_3)=\mathrm{rank}[\mathbf{t}_1,\mathbf{t}_2]=2=6-4$. In terms of bulk wave properties, the outmost equi-frequency surface of quadramode material is open in the $\mathbf{n}$ direction.

Under the elasticity tensor equation (3.22), there is no propagating Rayleigh wave in quadramode materials when $\mathrm{rank}(\mathbf{S}_3)=2$. Moreover, the displacement field of a Rayleigh mode for any $\mathrm{Re}(\xi)>0$ can also be expressed by equations (3.16) and (3.17).

When $\mathrm{rank}(\mathbf{S}_3)<2$, the outmost equi-frequency surface of quadramode materials is open in the $\mathbf{n}$ direction, resulting in wave property similar to that in a pentamode material. Then, the function Φ cannot be organized to the elegant form of (3.14). After discussing case by case in a similar way to appendix A, we may establish the same conclusion that the Rayleigh wave cannot propagate in quadramode materials when $\mathrm{rank}(\mathbf{S}_3)<2$. Details are omitted.

As a result, there is no propagating Rayleigh wave in a quadramode material.

(c) Other extremal materials

For a trimode material, i.e. $r=3, N=3$, using the same method as illustrated in quadramode materials, we can verify that no propagating Rayleigh wave exists when $\mathrm{rank}(\mathbf{S}_3)=\mathrm{rank}[\mathbf{t}_1,\mathbf{t}_2,\mathbf{t}_3]=3=6-3$. However, we find a special kind of trimode material that supports propagating Rayleigh waves when $\mathrm{rank}(\mathbf{S}_3)<3$, i.e. $\mathbf{t}_1$, $\mathbf{t}_2$ and $\mathbf{t}_3$ are linearly dependent.

Consider a trimode material, which is stiff to any stress in the (x, z)-plane and its hard modes are expressed by

$$\mathbf{S}^{(1)}=\sqrt{\mu}\begin{bmatrix} 1 & 0 & 0 \\ 0 & 0 & 0 \\ 0 & 0 & -1 \end{bmatrix},\ \mathbf{S}^{(2)}=\sqrt{\mu}\begin{bmatrix} 0 & 0 & 1 \\ 0 & 0 & 0 \\ 1 & 0 & 0 \end{bmatrix}\ \text{and}\ \mathbf{S}^{(3)}=\sqrt{\lambda+\mu}\begin{bmatrix} 1 & 0 & 0 \\ 0 & 0 & 0 \\ 0 & 0 & 1 \end{bmatrix}. \tag{3.23}$$

In equation (3.23), λ and μ are the Lamé constants. The CFVs are accordingly

$$\mathbf{t}_1=-\sqrt{\mu}[0,0,1]^T,\ \mathbf{t}_2=\sqrt{\mu}[1,0,0]^T\ \text{and}\ \mathbf{t}_3=\sqrt{\lambda+\mu}[0,0,1]^T, \tag{3.24}$$

with $\mathrm{rank}(\mathbf{S}_3)=2<3$. Such a trimode material is a three-dimensional orthotropic extremal material, possessing symmetry with respect to the (x, z)-plane. So, in (x, z)-plane, its elasticity matrix degenerates to a two-dimensional isotropic Cauchy material in Voigt or Kelvin notation

$$\mathbf{C}=\begin{bmatrix} \lambda+2\mu & \lambda & 0 \\ \lambda & \lambda+2\mu & 0 \\ 0 & 0 & \mu \end{bmatrix}. \tag{3.25}$$

The well-known Rayleigh equation for the phase velocity of Rayleigh waves in isotropic Cauchy materials can be expressed as [11]

$$\left(2-\frac{c^2}{c_T^2}\right)^2-4\left(1-\frac{c^2}{c_L^2}\right)^{\frac{1}{2}}\left(1-\frac{c^2}{c_T^2}\right)^{\frac{1}{2}}=0, \tag{3.26}$$

where $c_T=\sqrt{\mu/\rho}$ and $c_L=\sqrt{(\lambda+2\mu)/\rho}$ are transverse and longitudinal wave velocities, respectively. Substituting equations (3.25) into (3.26), the Rayleigh wave phase velocity and surface particles polarization may be obtained after some manipulations [11].

Next, for bimode ($r=4$, $N=2$) and unimode ($r=5$, $N=1$) materials, i.e. as the number of hard modes increases, it is even easier to construct a rank-sufficient elasticity matrix in the (x, z)-plane. In other words, Rayleigh waves may exist in certain crystal faces of bimode and unimode materials. For instance, in bimode and unimode materials, there always exist propagating Rayleigh waves in the (x, z)-plane, if three of the hard modes are in the form of equation (3.23).

In conclusion, there is no propagating Rayleigh wave in any three-dimensional pentamode and quadramode material. In addition, for trimode materials, Rayleigh waves exist only when $\mathrm{rank}(\mathbf{S}_3) = \mathrm{rank}[\mathbf{t}_1, \mathbf{t}_2, \mathbf{t}_3] < 3$. In unimode and bimode materials, Rayleigh waves exist in certain crystal faces where the two-dimensional degenerate elasticity matrix is rank-sufficient.

4. Application

In previous sections, we have demonstrated that there is no propagating Rayleigh wave in any two-dimensional extremal materials. The Rayleigh wave excited on the left side of an ordinary Cauchy material surface, as shown in figure 4c, is usually transmitted to the right side along the x-axis, even when it encounters another interlayer of ordinary Cauchy material. A Rayleigh wave may be blocked when it encounters an extremal material, since the extremal material does not support propagation of the Rayleigh waves. Therefore, the extremal materials may be adopted as a Rayleigh wave isolator. Compared with a hole dug to block the Rayleigh waves, extremal materials may withstand certain loads. In this section, we propose a Rayleigh wave isolator based on unimode material, and numerically demonstrate this for both homogenized and discrete models.

Numerical simulations are conducted by using the Solid Mechanics and Truss Module of commercial software package COMSOL Multiphysics 5.6 in the frequency domain with the multifrontal massively parallel sparse direction solver. In the simulation, the surroundings of the computed domain are covered by perfectly matched layers (PMLs) to eliminate wave reflection. Figure 4c shows the FEA model based on the homogenized material model to demonstrate the function of extremal material used as a Rayleigh wave isolator. The semi-infinite homogeneous material is aluminium with Lamé constants $\lambda_{Al} = 50.35\,\mathrm{GPa}$, $\mu_{Al} = 25.94\,\mathrm{GPa}$ and density $\rho_{Al} = 2700\,\mathrm{kg\,m^{-3}}$. A point source is used to excite the right-propagating Rayleigh wave on the free surface. The small rectangle on the middle right of the size length $20 \times 100\,\mathrm{mm}$ is filled with homogenized unimode material or ordinary Cauchy material, representing the interlayer inserted into the background medium. The Rayleigh wave propagation is calculated for these two cases separately to demonstrate the ability of the extremal material as a Rayleigh wave isolator. The same calculations are performed to check the designed unimode lattice and ordinary Cauchy lattice (as shown in figure 4a,b). The solid and lattice use uniform triangular meshes and bar element with meshes defined along the edge, respectively. In this case, the homogenized materials are respectively replaced by their corresponding lattice. The total size of the FEA model is $1200 \times 200\,\mathrm{mm}$.

Now we introduce two lattices for simulations. Consider a periodic pin-joint cubic symmetry truss model, with a unit cell sketched in figure 4a. All rods in the unit cell have the same length l and cross-sectional area A_{out}. Any neighbouring unit cell may be reached by translating the reference unit cell with a direct lattice translation vector $x_i\mathbf{a}_i$, with $i \in \{1, 2\}$, and $x_i \mathbb{Z}$. The Einstein summation rule is adopted for repeated indices. For the unit cell shown in figure 4a, we have

$$\mathbf{a}_1 = \left[\sqrt{2}l,\ 0\right]^T,\ \mathbf{a}_1 = \left[0,\ \sqrt{2}l\right]^T. \tag{4.1}$$

Then, the coordinates of the nodes are given by

$$\mathbf{n}_1 = \left[l/\sqrt{2},\ 0\right]^T,\ \mathbf{n}_2 = \left[0,\ l/\sqrt{2}\right]^T,\ \mathbf{n}_3 = \mathbf{n}_1 + \mathbf{a}_2,\ \mathbf{n}_4 = \mathbf{n}_2 + \mathbf{a}_1. \tag{4.2}$$

Following the Cauchy–Born hypothesis-based homogenization method (see [52] for details), this lattice can be homogenized as a unimode material with elasticity matrix

$$\mathbf{C}_{\mathrm{UM}} = \frac{E_b A_{\mathrm{out}}}{2l}\begin{bmatrix} 1 & 1 & 0 \\ 1 & 1 & 0 \\ 0 & 0 & 1 \end{bmatrix}, \tag{4.3}$$

in which E_b is Young's modulus of the rods. In addition, its effective mass density can be simply calculated by the volume average

$$\rho_{\mathrm{UM}}^{\mathrm{eff}} = \frac{2\rho_1 A_{\mathrm{out}}}{l}, \tag{4.4}$$

where ρ_1 is the mass density of rods in the unimode lattice.

Furthermore, by adding two red rods in the unit cell in figure 4a to construct a unit cell as shown in figure 4b, an ordinary Cauchy lattice (nullmode lattice, $N=0$) is obtained, with homogenized elasticity matrix

$$\mathbf{C}_{\mathrm{NM}} = \frac{E_b A_{\mathrm{out}}}{2l}\begin{bmatrix} 1+\sqrt{2}\bar{A} & 1 & 0 \\ 1 & 1+\sqrt{2}\bar{A} & 0 \\ 0 & 0 & 1 \end{bmatrix}. \tag{4.5}$$

Here, the normalized cross-sectional area is defined as $\bar{A} = A_{\mathrm{in}}/A_{\mathrm{out}}$, with A_{in} the cross-sectional area of the red rods. The effective mass density is

$$\rho_{\mathrm{NM}}^{\mathrm{eff}} = \frac{2\rho_2 A_{\mathrm{out}}}{l}\left(1+\frac{\bar{A}}{\sqrt{2}}\right), \tag{4.6}$$

where ρ_2 is the mass density of rods in the nullmode lattice. For microstructure lattice, the ideal material constants and geometric parameters are given unless otherwise explicitly specified: $E_b = 200\,\mathrm{GPa}$, $\rho_1 = 2\rho_2 = 1350\,\mathrm{kg\,m^{-3}}$, $l = 2\,\mathrm{mm}$, $A_{\mathrm{out}} = A_{\mathrm{in}}/\sqrt{2} = 2\times10^{-3}\mathrm{m}^2$. Then, the nullmode lattice is an isotropic Cauchy lattice, and the rectangular area is filled with 10×50 lattice unit cells. The homogenized elasticity matrix and densities of the unimode material and ordinary Cauchy materials are therefore

$$\mathbf{C}_{\mathrm{UM}} = \begin{bmatrix} 1 & 1 & 0 \\ 1 & 1 & 0 \\ 0 & 0 & 1 \end{bmatrix}\times 100\,\mathrm{GPa},\ \rho_{\mathrm{UM}}^{\mathrm{eff}} = \rho_{Al}, \tag{4.7}$$

$$\mathbf{C}_{NM} = \begin{bmatrix} 3 & 1 & 0 \\ 1 & 3 & 0 \\ 0 & 0 & 1 \end{bmatrix}\times 100\,\mathrm{GPa},\ \rho_{\mathrm{NM}}^{\mathrm{eff}} = \rho_{Al}. \tag{4.8}$$

Substituting the material constants of aluminium into (3.26), and after some manipulations [11], we obtain the Rayleigh wave phase velocity and surface particle polarization

$$c \approx 2869.05\ \mathrm{m\,s^{-1}},\ \hat{\mathbf{u}} = [0.5384,\ -0.8427\mathrm{i}]^T,\ \text{at } z=0. \tag{4.9}$$

Similarly, the Rayleigh wave in the isotropic material with elasticity matrix of equation (4.8) takes the phase velocity and surface particle polarization as

$$c \approx 5595.29\ \mathrm{m\,s^{-1}},\ \hat{\mathbf{u}} = [0.5630,\ -0.8264\mathrm{i}]^T,\ \text{at } z=0. \tag{4.10}$$

Since the two isotropic materials support different Rayleigh waves, when the material with equation (4.8) is inserted into the aluminium as an interlayer, to some extent, it will affect the propagation of Rayleigh waves in aluminium.

Figure 5 shows the simulation results of wave propagation in frequency domain, where the PMLs are not shown to illustrate more clearly the scattering fields. A right-propagating Rayleigh wave with frequency $f = 50\,\mathrm{kHz}$ and polarization equation (4.9) is excited from the left point source on the aluminium surface. The coloured contours represent the total displacement field normalized by the incident wave. Figure 5a$_1$,b$_1$ shows the simulation results for the interlayer

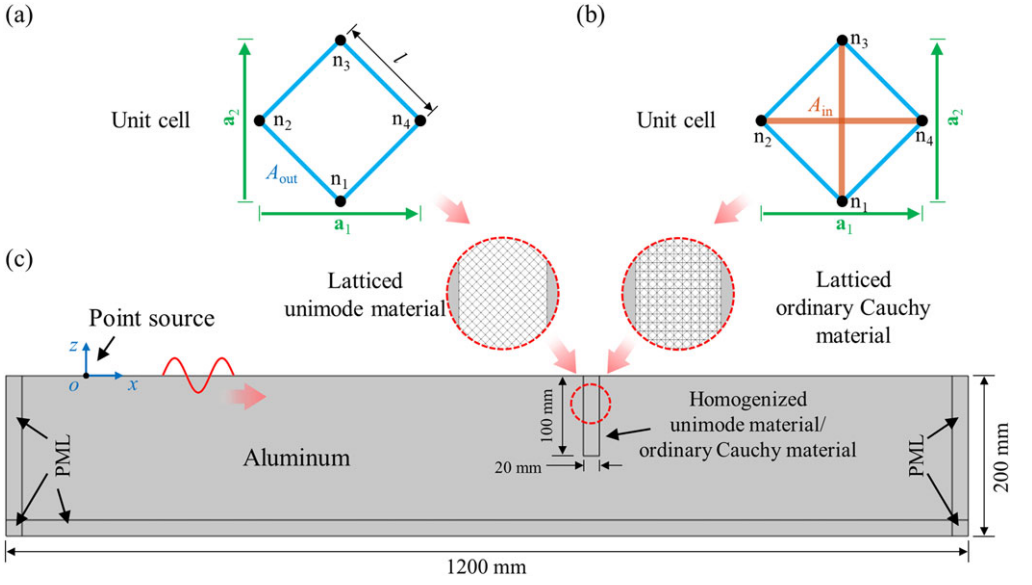

Figure 4. The sketch of unimode/Cauchy lattice and the finite-element analysis model in COMSOL. (a) Unimode lattice. The unit cell contains four nodes ($\mathbf{n}_1$ and $\mathbf{n}_2$ are independent nodes) and four rods. All of the rods in the unit cell have the same length l and the cross-sectional areas A_{out}. The a_i ($i = 1, 2$) is the direct translational basis. (b) Ordinary Cauchy lattice, same as (a) but add two red rods to connect the diagonal nodes. The cross-sectional area of red rods is A_{in}. (c) The simulation model consists of a piece of homogenized material of size 20 × 100 mm. The semi-infinite material is set to be aluminium and surrounded by PMLs on all boundaries except the top boundary (free surface). A point source is located at the middle left to excite Rayleigh waves. The middle right of the inserted interlayer may be the homogenized effective-medium or microstructure lattice.

employing the homogenized ordinary Cauchy material and homogenized unimode material, respectively. After the Rayleigh wave transmits through the piece of ordinary Cauchy material with equation (4.8), its amplitude decreases a little to the incident wave. However, when the ordinary Cauchy material is replaced by the unimode material with equation (4.7), it is clear that the Rayleigh wave is blocked to a large extent. This demonstrates the ability of extremal materials as a Rayleigh wave isolator, in agreement with the conclusion of no propagating Rayleigh wave supported in two-dimensional extremal materials for the continuum. Figure 5a_2,b_2 is the same calculations as figure 5a_1,b_1, but the homogenized materials are, respectively, replaced by their corresponding lattices. Consistency holds between the simulations and our conclusion for non-existence of Rayleigh waves in two-dimensional extremal materials. Furthermore, we compare the scattering fields between the homogenized model and the microstructure calculation (see the zoomed plot for clarity), i.e. figure 5a_1,a_2 as well as figure 5b_1,b_2. Again, we obtain a good agreement between the microstructure model and the effective-medium calculations. This, in fact, also confirms our designed microstructure for both the unimode material and the ordinary Cauchy material.

5. Summary

The exotic properties of Rayleigh wave in extremal materials, including its phase velocity and polarization of surface particles, have been examined in detail. To solve Rayleigh waves in extremal materials, we constructed a weak form with special test function. It is found that for most two-dimensional extremal materials, the kinetic energy of surface particles is always required to be zero, therefore these extremal materials do not support propagating Rayleigh waves. While, for other extremal two-dimensional materials, we proved case by case that neither

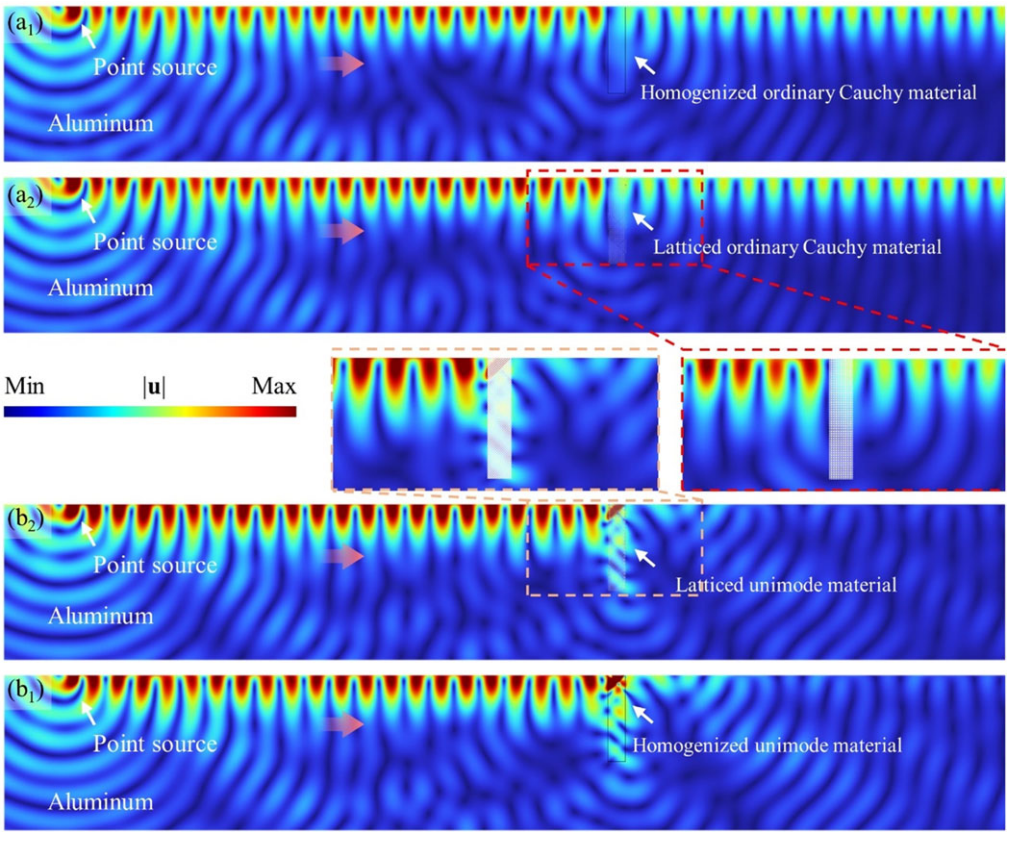

Figure 5. The normalized total displacement fields for illustrating the ability of extremal materials used as Rayleigh wave isolator. (a_1) and (b_1) are simulation results when the interlayer employing homogenized ordinary Cauchy material (with equation (4.8) and homogenized unimode material (with equation (4.7)), respectively. (a_2) and (b_2) are the same as (a_1) and (b_1) but the effective-media are replaced by ordinary Cauchy lattice and unimode lattice. Zoomed-in view plots the detail of the displacement field around the interlayer.

do they support such waves. In addition, during the proof in the three-dimensional case, it is also found that CFVs play an important role for Rayleigh wave properties in extremal materials. In short, Rayleigh waves do not propagate in any two-dimensional extremal elastic material. In three dimensions, pentamode and quadramode materials cannot support propagating Rayleigh wave. In contrast, we find a class of trimode materials satisfying $\mathrm{rank}(\mathbf{S}_3) < 3$ that support propagating the Rayleigh wave on a certain crystal face. However, when a trimode material satisfies $\mathrm{rank}(\mathbf{S}_3) = 3$, they do not support propagating Rayleigh wave in any crystal face. For bimode and unimode materials, Rayleigh waves may exist on certain crystal faces. Finally, a Rayleigh wave isolator is proposed and demonstrated. In two dimensions, it consists of unimode material, and numerical simulations are performed for both homogenized and corresponding discrete models. In summary, we provide a systematic study on Rayleigh waves in extremal materials in both two and three dimensions, paving the way for exploring the exotic wave properties of Rayleigh waves.

Data accessibility. This article has no additional data.

Declaration of AI use. We have not used AI-assisted technologies in creating this article.

Authors' contributions. B.W.: conceptualization, data curation, formal analysis, investigation, methodology, software, validation, visualization, writing—original draft, writing—review and editing; Y.W.: conceptualization, data curation, investigation, project administration, resources, software, visualization, writing—original draft, writing—review and editing; G.H.: conceptualization, formal analysis, funding

acquisition, investigation, methodology, project administration, resources, validation, writing—review and editing; S.T.: conceptualization, formal analysis, funding acquisition, investigation, methodology, project administration, supervision, validation, writing—review and editing.

All authors gave final approval for publication and agreed to be held accountable for the work performed therein.

Conflict of interest declaration. We declare we have no competing interests.

Funding. This research is partially supported by the National Natural Science Foundation of China under grants nos. (12588201, 11632003, 11972083 and 11991030).

Acknowledgements. The authors thank Prof. Yibin Fu and the anonymous reviewers for their stimulating discussions.

Appendix A

We first prove that there is no propagating Rayleigh wave in two-dimensional extremal materials when its elasticity matrix satisfies the constraint of $\det(\mathbf{T}) = 0$. The possible Rayleigh modes in this case are also calculated. Finally, an example of orthotropic extremal materials whose principle axis is θ to the coordinate axis is given to illustrate our findings.

Substituting equation (2.21) into equation (2.20) and discard the trivial case $\hat{\mathbf{A}}_1 = 0$, we get

$$\begin{aligned}(g\rho c^2 - a^2 g + fe)\xi + \mathrm{i}(d^2\rho c^2 - a^2 d^2 + f^2) = 0,\\ (d^2\xi + \mathrm{i}f)\rho c^2 = 0.\end{aligned} \tag{A 1}$$

Then, we have the following two circumstances: $c^2 = 0$ or $c^2 \neq 0$. We discuss the two cases separately.

The first circumstance $c^2 = 0$ indicates that the Rayleigh wave phase velocity is zero, i.e. there is no propagating Rayleigh waves. Considering $\mathrm{Re}(\xi)$ greater than 0, the relation of the coefficients can be simplified as

$$\det(\mathbf{T}) = \det(\mathbf{R}) = \det(\mathbf{Q}) = 0. \tag{A 2}$$

Here, equation (A 2) comes from equation (A 1). Then, in this case, the reduced elasticity matrix and Rayleigh mode for $\mathrm{Re}(\xi) > 0$ is

$$C = \begin{bmatrix} a^2 & ab & ad \\ ab & b^2 & bd \\ ad & bd & d^2 \end{bmatrix},\ \mathbf{u} = \begin{bmatrix} b\xi + \mathrm{i}d \\ -d\xi - \mathrm{i}a \end{bmatrix} \exp(\xi kz + \mathrm{i}kx),\ c = 0. \tag{A 3}$$

For $c^2 \neq 0$, according to equation (A 1), we get $d^2\xi + \mathrm{i}f = 0$. Since $\mathrm{Re}(\xi) > 0$, we have $d = f = 0$. Then, substituting $d = f = 0$ into the first equation in equation (2.21) leads to

$$g\hat{v}_1\xi = 0. \tag{A 4}$$

Therefore, we need either $\hat{v}_1 = 0$ or $\hat{v}_1 \neq 0$ for the traction-free condition.

For the first subcase, i.e. $\hat{v}_1 = 0$. Combining with the second equation in equation (2.21), we have $g\xi + \mathrm{i}e = 0$, then $g = e = 0$. After substituting $d = e = f = g = 0$ into equation (2.20), we get $\rho c^2 = a^2$. So, in this case, the elasticity matrix is reduced as

$$\mathbf{C}_0 = \mathrm{diag}(a^2,\ b^2,\ 0), \tag{A 5}$$

and the Rayleigh mode for any $\mathrm{Re}(\xi) > 0$ is

$$\mathbf{u} = \begin{bmatrix} \hat{u}_1 \\ 0 \end{bmatrix} \exp(\xi kz + \mathrm{i}k(x - ct)),\ \rho c^2 = a^2. \tag{A 6}$$

This is a rather special situation as the wave properties are similar to those of a material whose elastic tensor only has a non-zero component $C_{1111} = a^2$. It can be verified that the displacement field in equation (A 6) results in zero stress in the extremal materials. Since the wave properties

along the x-direction of extremal materials with elastic tensor of equation (A 5) behave like one-dimensional materials [44], the component C_{2222} are no use in this problem. Therefore, we discard this case, as we did in our previous work [56].

For the second subcase, i.e. $\hat{v}_1 \neq 0$. Then, according to equation (A 4), we have $g = 0$. After substituting $d = f = g = 0$ into equations (2.20) and (2.21), we get

$$\begin{aligned}(\rho c^2 - a^2)\hat{u}_1 &= -\mathrm{i}e\xi\hat{v}_1,\\ (\rho c^2 - d^2 + b^2\xi^2)\hat{v}_1 &= -\mathrm{i}e\xi\hat{u}_1,\\ b^2\xi\hat{v}_1 &= -\mathrm{i}e\hat{u}_1.\end{aligned} \tag{A 7}$$

From equation (A 7), we can solve $c = 0$ which contradicts with $c^2 \neq 0$.

In conclusion, there is no propagating Rayleigh wave exist in two-dimensional extremal materials when its elasticity matrix satisfies the constraint of $\det(\mathbf{T}) = 0$. In the following, two examples of orthotropic bimode extremal materials whose principle axis rotated by θ with respect to the coordinate axis are given to demonstrate our findings.

There are only two types of elasticity matrix $\mathbf{C}_0$ for orthotropic bimode extremal materials with $\det(\mathbf{T}) = 0$ [56]

$$\mathbf{C}_0 = \begin{bmatrix} a^2 & ab & 0\\ ab & b^2 & 0\\ 0 & 0 & 0\end{bmatrix}, \tag{A 8}$$

$$\mathbf{C}_0 = \mathrm{diag}(0,\ 0,\ d^2). \tag{A 9}$$

Then, the elasticity matrix $\mathbf{C}$ for the rotated orthotropic extremal material can be calculated by $\mathbf{C}_0$ combining equations (2.28) and (2.30).

We first consider the elasticity matrix of equation (A 8), which is basically an example of equation (A 3). Upon inserting equation (A 8) into equations (2.28) and (2.30), then into (A 3), we get the following wave modes for $\mathrm{Re}(\xi) > 0$

$$\mathbf{u} = \begin{bmatrix} (a\sin^2\theta + b\cos^2\theta)\xi + \mathrm{i}(a-b)\sin\theta\cos\theta\\ -(a-b)\xi\sin\theta\cos\theta - \mathrm{i}(a\cos^2\theta + b\sin^2\theta)\end{bmatrix}\exp(\xi kz + \mathrm{i}kx),\ c = 0. \tag{A 10}$$

The displacement field in equation (A 10) can be verified that it naturally satisfies the traction-free condition and therefore represents a Rayleigh mode in orthotropic bimode materials but with zero phase velocity for any θ.

Next, we consider the elasticity matrix of equation (A 9), which is also basically an example of equation (A 3). Similarly, we get

$$\mathbf{u} = \begin{bmatrix} \xi\sin 2\theta + \mathrm{i}\cos 2\theta\\ -\xi\cos 2\theta + \mathrm{i}\sin 2\theta\end{bmatrix}\exp(\xi kz + \mathrm{i}kx),\ c = 0, \tag{A 11}$$

which can be verified that it naturally satisfies the traction-free condition and therefore represents a Rayleigh mode but with zero phase velocity for any θ.

Note that, when $\theta = 0$, i.e. a bimode material whose principal axis is parallel to the free surface, equations (A 10) and (A 11) will be, respectively, reduced as

$$\mathbf{u} = \begin{bmatrix} b\xi\\ -\mathrm{i}a\end{bmatrix}\exp(\xi kz)\exp(\mathrm{i}k(x - ct)),\ c = 0,\ Re\{\xi\} > 0, \tag{A 12}$$

$$\mathbf{u} = \begin{bmatrix} \mathrm{i}\\ -\xi\end{bmatrix}\exp(\xi kz)\exp(\mathrm{i}k(x - ct)),\ c = 0,\ Re\{\xi\} > 0. \tag{A 13}$$

This is consistent with the results in our previous work [56].

References

1. Rayleigh L. 1885 On waves propagated along the plane surface of an elastic solid. *Proc. Lond. Math. Soc.* **1**, 4–11. (doi:10.1112/plms/s1-17.1.4)
2. Shapiro NM, Campillo M. 2004 Emergence of broadband Rayleigh waves from correlations of the ambient seismic noise. *Geophys. Res. Lett.* **31**, 7. (doi:10.1029/2004GL019491)
3. Xia JH, Miller RD, Park CB, Ivanov J, Tian G, Chen C. 2004 Utilization of high-frequency Rayleigh waves in near-surface geophysics. *Leading Edge* **23**, 753–759. (doi:10.1190/1.1786895)
4. Shui G, Kim JY, Qu J, Wang YS, Jacobs LJ. 2008 A new technique for measuring the acoustic nonlinearity of materials using Rayleigh waves. *NDT & E Int.* **41**, 326–329. (doi:10.1016/j.ndteint.2008.01.007)
5. Nazarian S, Stokoe II KH, Hudson WR. 1983 Use of spectral analysis of surface waves method for determination of moduli and thicknesses of pavement systems. *Transport. Res. Rec.* **930**, 38–45.
6. Achenbach JD. 2000 Quantitative nondestructive evaluation. *Int. J. Solids Struct.* **37**, 13–27. (doi:10.1016/S0020-7683(99)00074-8)
7. Schneider D, Schwarz T, Scheibe HJ, Panzner M. 1997 Non-destructive evaluation of diamond and diamond-like carbon films by laser induced surface acoustic waves. *Thin Solid Films* **295**, 107–116. (doi:10.1016/S0040-6090(96)09163-8)
8. Hobiger M *et al.* 2013 Ground structure imaging by inversions of Rayleigh wave ellipticity: sensitivity analysis and application to European strong-motion sites. *Geophys. J. Int.* **192**, 207–229. (doi:10.1093/gji/ggs005)
9. Love AEH. 2013 *A treatise on the mathematical theory of elasticity*. Cambridge, UK: Cambridge University Press.
10. Stroh AN. 1962 Steady state problems in anisotropic elasticity. *J. Math. Phys.* **41**, 77–103. (doi:10.1002/sapm196241177)
11. Achenbach JD. 2012 *Wave propagation in elastic solids*. New York, NY: Elsevier, North-Holland.
12. Auld BA. 1990 *Acoustic fields and waves in solids*, 2nd edn. Malabar, India: Krieger Publishing Company.
13. Rose JL. 1999 *Ultrasonic guided waves in solid media*. Cambridge, UK: Cambridge University Press.
14. Eringen AC. 2012 *Microcontinuum field theories: I. Foundations and solids*. New York, NY: Springer Science & Business Media.
15. Barnett DM, Lothe J. 1973 Synthesis of the sextic and the integral formalism for dislocations, Green's functions, and surface waves in anisotropic elastic solids. *Physic. Norvegica.* **17**, 13–19.
16. Barnett DM, Lothe J. 1985 Free surface (Rayleigh) waves in anisotropic elastic half-spaces: the surface impedance method. *Proc. R. Soc. Lond. A* **402**, 135–152. (doi:10.1098/rspa.1985.0111)
17. Lothe J, Barnett DM. 1976 On the existence of surface-wave solutions for anisotropic half-spaces with free surface. *J. Appl. Phys.* **47**, 428–433. (doi:10.1063/1.322665)
18. Chadwick P, Smith GD. 1977 Foundations of the theory of surface waves in anisotropic elastic materials. *Adv. Appl. Phys.* **17**, 303–376. (doi:10.1016/S0065-2156(08)70223-0)
19. Pal RK, Ruzzene M. 2017 Edge waves in plates with resonators: an elastic analogue of the quantum valley Hall effect. *New J. Phys.* **19**, 25001. (doi:10.1088/1367-2630/aa56a2)
20. Chen H, Nassar H, Huang GL. 2018 A study of topological effects in 1D and 2D mechanical lattices. *J. Mech. Phys. Solids* **117**, 22. (doi:10.1016/j.jmps.2018.04.013)
21. Chen Y, Liu X, Hu G. 2019 Topological phase transition in mechanical honeycomb lattice. *J. Mech. Phys. Solids* **122**, 54. (doi:10.1016/j.jmps.2018.08.021)
22. Chen Y, Zhang Q, Zhang Y, Xia B, Liu X, Zhou X, Chen C, Hu G. 2021 Research progress of elastic topological materials. *Adv. Mech.* **51**, 189–256. (doi:10.6052/1000-0992-21-015)
23. Zhang Q, Chen Y, Zhang K, Hu G. 2019 Programmable elastic valley Hall insulator with tunable interface propagation routes. *Extreme Mech. Lett.* **28**, 76–80. (doi:10.1016/j.eml.2019.03.002)
24. Zhang Q, Chen Y, Zhang K, Hu G. 2020 Dirac degeneracy and elastic topological valley modes induced by local resonant states. *Phys. Rev. B* **101**, 014101. (doi:10.1103/PhysRevB.101.014101)
25. Zhao YC, Zhou XM, Huang GL. 2020 Non-reciprocal Rayleigh waves in elastic gyroscopic medium. *J. Mech. Phys. Solids* **143**, 104065. (doi:10.1016/j.jmps.2020.104065)
26. Palermo A, Celli P, Yousefzadeh B, Daraio C, Marzani A. 2020 Surface wave non-reciprocity via time-modulated metamaterials. *J. Mech. Phys. Solids* **145**, 104181. (doi:10.1016/j.jmps.2020.104181)

27. Asbóth JK, Oroszlány L, Pályi A. 2016 A short course on topological insulators. *Lect. Notes Phys.* **919**, 997. (doi:10.1063/1.322665)
28. Scheibner C, Souslov A, Banerjee D, Surówka P, Irvine W, Vitelli V. 2020 Odd elasticity. *Nat. Phys.* **16**, 475–480. (doi:10.1038/s41567-020-0795-y)
29. Cheng W, Hu GK. 2021 Odd elasticity realized by piezoelectric material with linear feedback. *Sci. China Phys. Mech.* **64**, 1–10. (doi:10.1007/s11433-021-1755-6)
30. Nassar H, Chen YY, Huang GL. 2018 A degenerate polar lattice for cloaking in full two-dimensional elastodynamics and statics. *Proc. R. Soc. A* **474**, 20180523. (doi:10.1098/rspa.2018.0523)
31. Nassar H, Chen YY, Huang GL. 2019 Isotropic polar solids for conformal transformation elasticity and cloaking. *J. Mech. Phys. Solids* **129**, 229–243. (doi:10.1016/j.jmps.2019.05.002)
32. Zhang HK, Chen Y, Liu XN, Hu GK. 2020 An asymmetric elastic metamaterial model for elastic wave cloaking. *J. Mech. Phys. Solids* **135**, 103796. (doi:10.1016/j.jmps.2019.103796)
33. Fang N, Xi D, Xu J, Ambati M, Srituravanich W, Sun C, Zhang X. 2006 Ultrasonic metamaterials with negative modulus. *Nat. Mater.* **5**, 452–456. (doi:10.1038/nmat1644)
34. Liu XN, Hu GK, Huang GL, Sun CT. 2011 An elastic metamaterial with simultaneously negative mass density and bulk modulus. *Appl. Phys. Lett.* **98**, 251907. (doi:10.1063/1.3597651)
35. Zhu R, Liu XN, Hu GK, Sun CT, Huang GL. 2014 Negative refraction of elastic waves at the deep-subwavelength scale in a single-phase metamaterial. *Nat. Commun.* **5**, 1–8. (doi:10.1038/ncomms6510)
36. Milton GW, Cherkaev AV. 1995 Which elasticity tensors are realizable? *ASME J. Eng. Mater. Technol.* **117**, 483–493. (doi:10.1115/1.2804743)
37. Milton GW. 2002 *The theory of composites*. Cambridge, UK: Cambridge University Press. xxviiiþ719 pp. LCCNTA418.9.C6M58 2001.
38. Kadic M, Bückmann T, Stenger N, Thiel M, Wegener M. 2012 On the practicability of pentamode mechanical metamaterials. *Appl. Phys. Lett.* **100**, 191901. (doi:10.1063/1.4709436)
39. Kadic M, Bückmann T, Schittny R, Gumbsch P, Wegener M. 2014 Pentamode metamaterials with independently tailored bulk modulus and mass density. *Phys. Rev. Appl.* **2**, 54007. (doi:10.1103/PhysRevApplied.2.054007)
40. Zheng MY, Liu XN, Chen Y, Miao HC, Zhu R, Hu GK. 2019 Theory and realization of nonresonant anisotropic singly polarized solids carrying only shear waves. *Phys. Rev. Appl.* **12**, 014027. (doi:10.1103/PhysRevApplied.12.014027)
41. Dong H, Zhao S, Miao X, Shen C, Zhang X, Zhao Z, Zhang C, Wang Y, Cheng L. 2021 Customized broadband pentamode metamaterials by topology optimization. *J. Mech. Phys. Solids* **152**, 104407. (doi:10.1016/j.jmps.2021.104407)
42. Groß MF, Schneider JL, Chen Y, Kadic M, Wegener M. 2023 Dispersion engineering by hybridizing the back-folded soft mode of monomode elastic metamaterials with stiff acoustic modes. *Adv. Mater.* **36**, 2307553. (doi:10.1002/adma.202307553)
43. Zhang HK, Kang Z, Wang YQ, Wu WJ. 2020 Isotropic 'quasi-fluid' metamaterials designed by topology optimization. *Adv. Theor. Simul.* **3**, 1900182. (doi:10.1002/adts.201900182)
44. Wei Y, Hu GK. 2022 Wave characteristics of extremal elastic materials. *Extreme Mech. Lett.* **55**, 101789. (doi:10.1016/j.eml.2022.101789)
45. Chen Y, Zheng MY, Liu XN, Bi YF, Sun ZY, Xiang P, Yang J, Hu GK. 2017 Broadband solid cloak for underwater acoustics. *Phys. Rev. B* **95**, 180104. (doi:10.1103/PhysRevB.95.180104)
46. Norris AN. 2009 Acoustic metafluids. *J. Acoust. Soc. Am.* **125**, 839. (doi:10.1121/1.3050288)
47. Zheng MY, Park CII, Liu XN, Zhu R, Hu GK, Kim YY. 2020 Non-resonant metasurface for broadband elastic wave mode splitting. *Appl. Phys. Lett.* **116**, 171903. (doi:10.1063/5.0005408)
48. Cheng W, Zhang HK, Wei Y, Wang K, Hu GK. 2024 Elastic energy and polarization transport through spatial modulation. *J. Mech. Phys. Solids* **182**, 105475. (doi:10.1016/j.jmps.2023.105475)
49. Wei Y, Liu XN, Hu GK. 2021 Quadramode materials: their design method and wave property. *Mater. Design* **210**, 110031. (doi:10.1016/j.matdes.2021.110031)
50. Groß MF, Schneider JLG, Wei Y, Chen Y, Kalt S, Kadic M, Liu X, Hu G, Wegener M. 2023 Tetramode metamaterials as phonon polarizers. *Adv. Mater.* **35**, 2211801. (doi:10.1002/adma.202211801)
51. Bückmann T, Thiel M, Kadic M, Schittny R, Wegener M. 2014 An elasto-mechanical unfeelability cloak made of pentamode metamaterials. *Nat. Commun.* **5**, 1–6. (doi:10.1038/ncomms5130)
52. Wei Y, Cai M, Hu GK. 2024 Elastic birefringent metamaterials and quarter-wave plate. *Int. J. Mech. Sci.* **281**, 109684. (doi:10.1016/j.ijmecsci.2024.109684)

53. Chen Y, Zhao BH, Liu XN, Hu GK. 2020 Highly anisotropic hexagonal lattice material for low frequency water sound insulation. *Extreme Mech. Lett.* **40**, 100916. (doi:10.1016/j.eml.2020.100916)
54. Wang DW, Zhao BH, Wei Y, Yang J, Hu GK. 2024 Material design for hydraulic silencers. *Phys. Rev. Appl.* **22**, 034010. (doi:10.1103/PhysRevApplied.22.034010)
55. Fraternali F, Amendola A. 2017 Mechanical modeling of innovative metamaterials alternating pentamode lattices and confinement plates. *J. Mech. Phys. Solids* **99**, 259–271. (doi:10.1016/j.jmps.2016.11.010)
56. Wei Y, Chen Y, Cheng W, Liu XN, Hu GK. 2024 Rayleigh surface waves of extremal elastic materials. *J. Mech. Phys. Solids* **193**, 105842. (doi:10.1016/j.jmps.2024.105842)
57. Stroh AN. 1958 Dislocations and cracks in anisotropic elasticity. *Phil. Mag.* **3**, 625. (doi:10.1080/14786435808565804)
58. Ting TCT. 1996 *Anisotropic elasticity, theory and applications*. New York, NY: Oxford University Press.
59. Fu YB, Mielke A. 2002 A new identity for the surface–impedance matrix and its application to the determination of surface-wave speeds. *Proc. R. Soc. A* **458**, 2523–2543. (doi:10.1098/rspa.2002.1000)
60. Malischewsky PG, Scherbaum F. 2004 Love's formula and *H/V*-ratio (ellipticity) of Rayleigh waves. *Wave Motion* **40**, 57–67. (doi:10.1016/j.wavemoti.2003.12.015)
61. Ting TCT, Barnett DM. 1997 Classifications of surface waves in anisotropic elastic materials. *Wave Motion* **26**, 207–218. (doi:10.1016/S0165-2125(97)00027-9)
62. Barnett DM. 2000 Bulk, surface, and interfacial waves in anisotropic linear elastic solids. *Int. J. Solids Struct.* **37**, 45–54. (doi:10.1016/S0020-7683(99)00076-1)